Driving convection in a fluid layer by a temperature gradient or a heat current

P. Matura and M. Lücke
Institut für Theoretische Physik, Universität des Saarlandes, D-66041 Saarbrücken, Germany
(Received 9 June 2005; published 15 March 2006)

Bifurcation properties, stability behavior, dynamics, and the heat transfer of convection in a horizontal fluid layer that is driven away from thermal equilibrium by imposing a vertical temperature difference are compared with those resulting from imposing a heat current. Similarities and differences are elucidated. In particular various paradigmatic backwards bifurcating convection structures that occur, e.g., in binary fluid mixtures are determined numerically for the two different driving mechanisms. Conditions are given under which current driven convection is stable when temperature driven convection is unstable.

DOI: 10.1103/PhysRevE.73.037301 PACS number(s): 47.20.Ky, 47.27.te, 47.54.−r

Many nonlinear dissipative systems that are driven away from thermal equilibrium show self-organization out of an unstructured state: A structured one appears when the driving exceeds a critical threshold [1]. The driving might be realized by imposing a field gradient across the system—e.g., a voltage difference across a semiconductor [2] or a liquid crystal [3], a temperature difference across a fluid layer [4], or a concentration difference in a physical [5], chemical [6], or biological [7] system—which drives a current. Or, alternatively, a current might be injected at one side of the system [8–10]. Now the question is, whether and how the dissipative structures that form in response to these two different driving mechanisms are related to each other concerning their dynamics, their structure, their stability behavior, and their bifurcation properties.

It is surprising that this question has not yet been studied extensively for the paradigmatic, abundant, and easy accessible convective structures in horizontal fluid layers heated from below [11,12]. Even more so since up to about the end of the 1980's convection experiments were done with imposed heat current at the lower plate. On the other hand, (servo) control of both plate's temperatures seems to have been realized only later, partly at the request of theorists who favored Dirichlet boundary conditions.

We have investigated this question numerically for convection in a binary fluid such as, e.g., ethanol-water as a representative example since there are a variety of different structures that may be studied quantitatively already at a small driving [1,13,14]: There are spatially extended states of stationary convection rolls and of temporally oscillating roll patterns in the form of traveling waves (TWs) and of standing waves (SWs) that bifurcate forwards or backwards out of the quiescent fluid state. In addition there are also spatially localized traveling wave states that compete with extended convection structures.

Here, we focus on convection in the form of straight parallel rolls as they occur, e.g., in narrow channels with roll axes perpendicular to the long side walls. We have solved the appropriate hydrodynamic field equations [13,15] with a finite-differences method [16] in a vertical x-z cross section through the rolls perpendicular to their axes thus ignoring effects that come from field variations along the roll axes [13,17,18].

Calculations were done for ethanol-water parameters, Lewis number $L=0.01$ and Prandtl number $\sigma=10$. Results are presented here for two different separation ratios $\psi=-0.03$ and $\psi=-0.1$ [19,20] for which TW and SW solutions bifurcate subcritically out of the quiescent fluid state via a common Hopf bifurcation. Our findings concerning the above posed questions are representative also for TWs and SWs at stronger, i.e., more negative Soret coupling strength ψ.

The horizontal boundaries at top ($z=1$) and bottom ($z=0$) are no slip, impermeable, and perfectly heat conducting, thus enforcing the absence of lateral temperature gradients there. Sapphire or copper plates provide a good experimental approximation. Two different experimentally realizable horizontal boundary conditions (bc) for the temperature are explored here: (i) Dirichlet bc of fixed temperatures (constant in space and time) at $z=0$ and $z=1$ with a difference of ΔT between them and (ii) von Neumann bc of fixed total vertical heat current at $z=0$ and Dirichlet bc of fixed temperature at

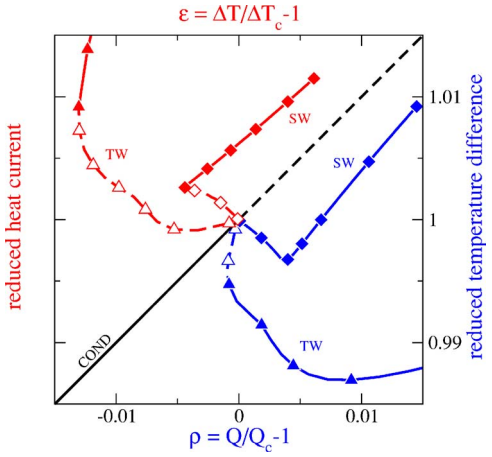

FIG. 1. (Color online) Bifurcation diagrams of heat current and temperature difference for oscillatory convection at $\psi=-0.03$ subject to different bc. The upper left (lower right) part shows $Q/Q_c(\Delta T/\Delta T_c)$ for TT (QT) driving versus $\epsilon(\rho)$ on the upper (lower) abscissa. For SWs the time averages $\langle Q\rangle/Q_c$ and $\langle \Delta T\rangle/\Delta T_c$, respectively, are plotted. The bisecting line marks the quiescent conductive state. Full (dashed) lines and filled (open) symbols denote stable (unstable) states. SW solutions were obtained with phase pinning conditions; otherwise they are completely unstable.

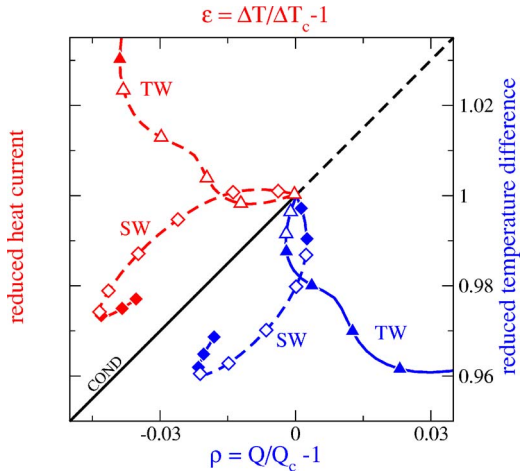

FIG. 2. (Color online) Bifurcation diagrams of heat current and temperature difference as in Fig. 1. Here, however, for $\psi=-0.1$.

$z=1$. At the impermeable boundaries the vertical concentration current vanishes and consequently the local vertical heat current reduces there to $-\partial_z T$ [15]. Note that we impose in case (ii) the horizontal mean

$$Q = -\overline{\partial_z T|_{z=0}} \tag{1}$$

of the heat current at the lower side of the fluid layer so that the total heat current injected into it is a constant. We refer to the driving conditions of the case (i) as TT and to those of case (ii) as QT.

Laterally we impose for all fields periodic bc with wavelength $\lambda=2$. This is roughly the critical one for onset of oscillatory convection. Moreover, it is often seen also in nonlinear convection with rolls of about circular shape. Finally, to determine SW solutions that are unstable against horizontal mirror symmetry breaking phase propagation we enforce horizontal mirror symmetry, say, at $x=0$ thereby fixing the phase [21].

As control parameter measuring the strength of the driving we use in the TT case the relative deviation

$$\epsilon = \Delta T/\Delta T_c - 1 \tag{2}$$

from the critical temperature difference ΔT_c for onset of convection. The driving in case QT is measured by the relative deviation

$$\rho = Q/Q_c - 1 \tag{3}$$

from the critical imposed heat current.

We shall discuss first TW convection and then SW solutions. In Figs. 1 and 2 we show for two different ψ the bifurcation diagrams of nonlinear relaxed TW states: (i) current Q as a function of ϵ for TT driving and (ii) temperature difference ΔT versus ρ for the QT case. Note that Q as well as ΔT are constant for TWs. The diagonal line shows the

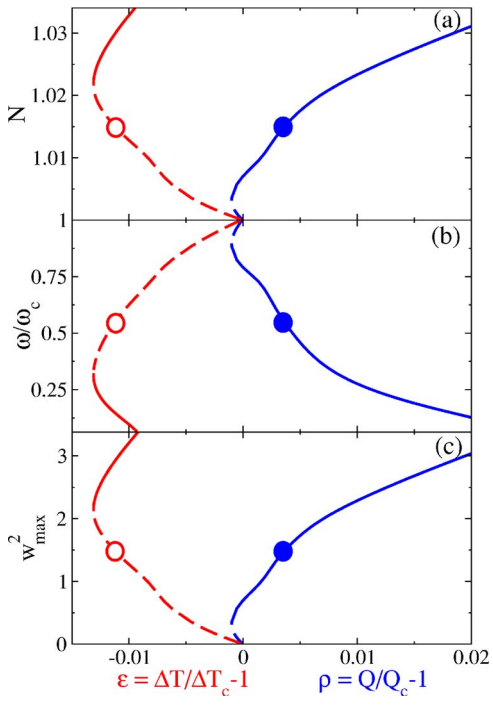

FIG. 3. (Color online) TW bifurcation diagrams: (a) Nusselt number N, (b) reduced oscillation frequency ω/ω_c, and (c) squared maximal vertical velocity w_{max}^2 for the TWs of Fig. 1 with $\psi=-0.03$. The left and right curves refer to TT and QT driving, respectively. Full (dashed) lines denote stable (unstable) TWs. Symbols identify examples of equivalent TWs for equivalent control parameters ϵ and ρ.

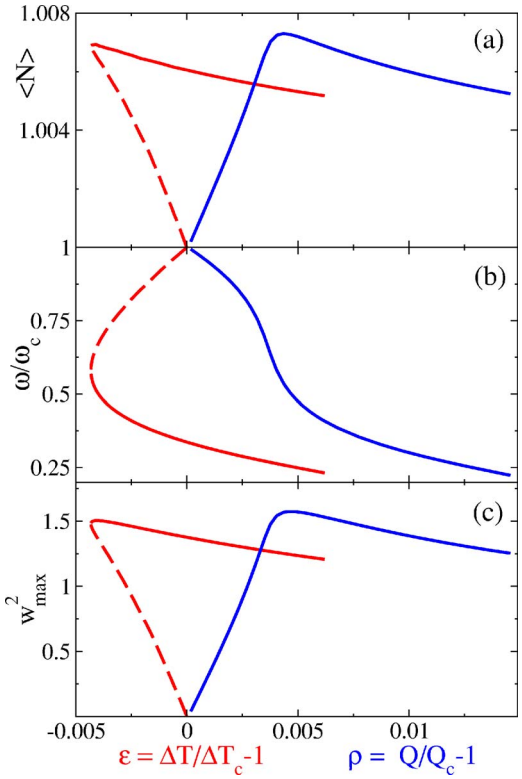

FIG. 4. (Color online) SW bifurcation diagrams: (a) time averaged Nusselt number $\langle N\rangle$, (b) reduced oscillation frequency ω/ω_c, and (c) squared maximal vertical velocity w_{max}^2 for the SWs of Fig. 1 with $\psi=-0.03$. The left and right curves refer to TT and QT driving, respectively. Full (dashed) lines denote stable (unstable) SWs.

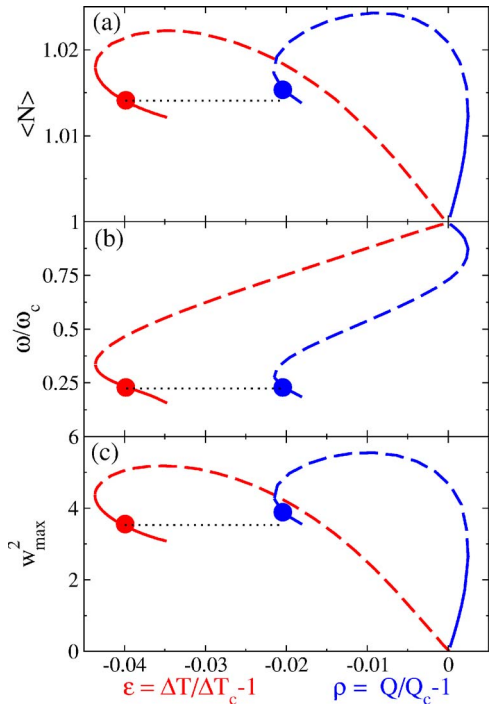

FIG. 5. (Color online) SW bifurcation diagrams as in Fig. 4 but for the SWs of Fig. 2 with $\psi=-0.1$. Symbols identify examples of SWs with the same frequency.

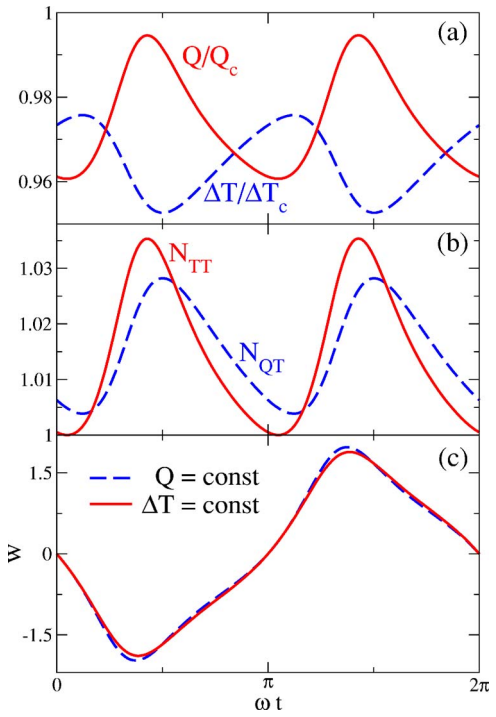

FIG. 6. (Color online) Oscillation profiles of the SWs marked in Fig. 5 by symbols. (a) Current and temperature oscillation subject to TT and QT driving, respectively. (b) Nusselt numbers $N_{TT}(t)=[Q(t)/Q_c]\Delta T_c/\Delta T=Q(t)/Q_{cond}$ and $N_{QT}(t)=(Q/Q_c)[\Delta T_c/\Delta T(t)]=\Delta T_{cond}/\Delta T(t)$. (c) Vertical velocity w at midheight between two rolls.

linear diffusive relation $Q_{cond}/Q_c=\Delta T_{cond}/\Delta T_c$ of the quiescent conductive state. It loses stability via a Hopf bifurcation at ΔT_c or Q_c, respectively. After increasing the driving slightly beyond this threshold transient growth of oscillatory convection occurs with increasing Q for the TT case. For QT conditions ΔT decreases since convection cools the lower boundary. Initially, the oscillations have the Hopf frequency. But finally, the TT transient ends in a stationary convection state since the TW branch terminates with zero frequency in a stationary solution branch already below $\epsilon=0$ for our ψ's [22]. On the other hand, the QT growth transient ends in a relaxed nonlinear TW (lower part of Figs. 1 and 2).

The curves of Q/Q_c versus ϵ and of $\Delta T/\Delta T_c$ versus ρ in Figs. 1 and 2 are reflections of each other at the diagonal, bisecting conduction line. Note, however, that the transients and the stability ranges of the relaxed TWs are different. Concerning the latter, for example, the hysteresis interval in ρ for QT is significantly smaller than the one in ϵ for TT since a large portion of unstable TT generated TWs below onset gets stabilized under QT driving.

In Fig. 3 we show for the TWs of Fig. 1 bifurcation diagrams of Nusselt number N, reduced frequency ω/ω_c, and squared maximal vertical velocity w_{max}^2 versus the respective control parameters. The Nusselt number

$$N=Q/Q_{cond}=(Q/Q_c)\Delta T_c/\Delta T \tag{4}$$

provides the relation

$$\rho=(1+\epsilon)N-1 \tag{5}$$

between equivalent control parameters ϵ and ρ corresponding to reflection at the conductive diagonal in Figs. 1 and 2: TWs that are generated by TT or QT driving at ϵ- and ρ-values related by (5) have the same spatiotemporal properties, e.g., the same N,ω,w_{max} as indicated by the symbols in Fig. 3. Their stability, however, might differ.

Equation (5) yields also the relation

$$\partial_\rho A=\partial_\epsilon A/[N+(1+\epsilon)\partial_\epsilon N] \tag{6}$$

between the slopes $\partial_\rho A(\rho)$ and $\partial_\epsilon A(\epsilon)$ in the QT and TT bifurcation diagrams of any order parameter A (say, N,ω,w_{max}^2, etc.) versus ρ or ϵ, respectively. Hence, the QT bifurcation becomes already tricritical, i.e., it changes from backwards to forwards when the initial slope $s=\partial_\epsilon N(\epsilon=0)$ of the TT Nusselt number increases beyond -1. In other words, all TT driven backwards bifurcating unstable TWs for which $s>-1$ can be stabilized by switching over to QT driving.

Note that the relations (5) and (6) hold also for any stationary convection solution so that the bifurcation diagrams of Q/Q_c versus ϵ and of $\Delta T/\Delta T_c$ versus ρ are reflections of each other. Thus, the stabilization effect of QT driving holds also for any stationary convection that bifurcates backwards with TT [23,24]. The (stability) properties of forward bifurcating stationary convection remain unchanged when using QT instead of TT conditions.

In the remainder of this paper we discuss SW convection. Under TT (QT) driving the heat current Q (temperature difference ΔT) oscillates with twice the SW frequency [25]. So, in Figs. 1 and 2 we show bifurcation diagrams of the time averages $\langle Q\rangle/Q_c$ and $\langle\Delta T\rangle/\Delta T_c$, respectively. Such as for

TWs, QT conditions have a stabilizing effect also on SWs. Note, however, that the two SW solution branches in these figures are not reflections of each other at the conduction diagonal. Their spatiotemporal properties differ and the relation $\langle\rho\rangle=(1+\epsilon)\langle N\rangle-1$ provides only an approximate equivalence between the bifurcation diagrams of the order parameters in Figs. 4 and 5. For example, the SWs marked by symbols in Fig. 5 have the same frequency. But w_{max} differs slightly and so does $\langle N\rangle$—i.e., $\langle Q/Q_c\rangle\Delta T_c/\Delta T$ for TT driving in comparison with $(Q/Q_c)\langle\Delta T_c/\Delta T\rangle$ for QT driving. Also the oscillations of the flow differ slightly [Fig. 6(c)]. On the other hand, the oscillation profile of $Q(t)$ differs significantly from the one of $\Delta T(t)$ [Fig. 6(a)] and also the profile of $N_{TT}(t)$ differs from the one of $N_{QT}(t)$ [Fig. 6(b)].

We elucidated similarities and differences in the nonequilibrium response of a structure forming system to an imposed field gradient or to an injected current for the paradigmatic example of binary mixture convection. Fixing the injected heat current can stabilize backwards bifurcating solutions, e.g., SW, TW, or stationary states, that are unstable with imposed temperature difference. However, irrespective of their stability structures that sustain a time independent current in the bulk (like TW and stationary convection) are simply related to each other for the two different boundary conditions. But time dependent solutions—such as, e.g., growth transients or in particular relaxed SW oscillations—differ in general. Thus, it would be interesting to see how far these different driving conditions influence the spatiotemporal properties of convection structures with more complex dynamics in whatever system they occur.

[1] M. C. Cross and P. C. Hohenberg, Rev. Mod. Phys. **65**, 851 (1993); and references cited therein.

[2] E. Schöll, F. J. Niedernostheide, J. Parisi, W. Prettl, and H. G. Purwins, in *Evolution of Structures in Dissipative Continuous Systems*, edited by F. H. Busse and S. C. Müller, Lecture Notes in Physics, m55 (Springer, Berlin, 1998), p. 446; E. Schöll, *Nonlinear Spatio-Temporal Dynamics and Chaos in Semiconductors* (Cambridge University Press, Cambridge, 2001); and references cited therein.

[3] *Pattern Formation in Liquid Crystals*, edited by A. Buka and L. Kramer (Springer, Berlin, 1996).

[4] E. Bodenschatz, W. Pesch, and G. Ahlers, Annu. Rev. Fluid Mech. **32**, 709 (2000).

[5] A. A. Predtechensky, W. D. McCormick, J. B. Swift, Z. Noszticzius, and H. L. Swinney, Phys. Rev. Lett. **72**, 218 (1994); N. Tsitverblit, Phys. Lett. A **329**, 445 (2004).

[6] Y. Kuramoto, *Chemical Oscillations, Waves and Turbulence* (Courier Dover Publications, New York, 2003).

[7] S. Camazine, J. L. Deneubourg, N. R. Franks, J. Sneyd, G. Theraula, and E. Bonabeau, *Self-Organization in Biological Systems* (Princeton University Press, Princeton, 2003).

[8] G. Ahlers, Phys. Rev. Lett. **33**, 1185 (1974); R. P. Behringer and G. Ahlers, J. Fluid Mech. **125**, 219 (1982); G. Ahlers and I. Rehberg, Phys. Rev. Lett. **56**, 1373 (1986).

[9] R. W. Walden, P. Kolodner, A. Passner, and C. M. Surko, Phys. Rev. Lett. **55**, 496 (1985).

[10] E. Moses and V. Steinberg, Phys. Rev. A **34**, R693 (1986).

[11] Early experiments done with an isopropanol-water mixture in two different setups showed different hysteresis loops in Schmidt-Milverton plots of temperature difference (on the ordinate) versus heat current (on the abscissa) depending on which of the two was imposed [12].

[12] D. Villers and J. K. Platten, J. Non-Equilib. Thermodyn. **9**, 131 (1984).

[13] J. K. Platten and J. C. Legros, *Convection in Liquids* (Springer, Berlin, 1984).

[14] M. Lücke, W. Barten, P. Büchel, C. Fütterer, St. Hollinger, and Ch. Jung, in *Evolution of Structures in Dissipative Continuous Systems*, edited by F. H. Busse and S. C. Müller, Lecture Notes in Physics, m55 (Springer, Berlin, 1998), p. 127.

[15] L. D. Landau and E. M. Lifshitz, *Fluid Mechanics* (Pergamon Press, Oxford, 1987).

[16] W. Barten, M. Lücke, M. Kamps, and R. Schmitz, Phys. Rev. E **51**, 5636 (1995).

[17] A. Alonso and O. Batiste, Theor. Comput. Fluid Dyn. **18**, 239 (2004).

[18] Ch. Jung, Ph.D thesis, Universität des Saarlandes (1997).

[19] For 1.4 weight % of ethanol mixed into water at $T=20\,^{\circ}\mathrm{C}$ the separation ratio measuring the Soret coupling strength between temperature and concentration gradients is $\psi\simeq-0.1$ [18,20].

[20] P. Kolodner, H. L. Williams, and C. Moe, J. Chem. Phys. **88**, 6512 (1988).

[21] P. Matura, D. Jung, and M. Lücke, Phys. Rev. Lett. **92**, 254501 (2004).

[22] St. Hollinger and M. Lücke, Phys. Rev. E **57**, 4238 (1998).

[23] Pure fluids with temperature dependent material parameters that are showing a stationary backwards bifurcation for TT driving were predicted [24] to allow oscillations under QT conditions. But we did not find such a behavior in our system.

[24] F. H. Busse, J. Fluid Mech. **28**, 223 (1967).

[25] For TT driving the laterally integrated currents at $z=0$ and $z=1$ oscillate in a SW in phase as a consequence of a mirror-glide symmetry [14,21]: $\delta T(x,z,t)=-\delta T(x+\lambda/2,1-z,t)$ holds for the temperature deviation from the mean. For QT conditions the temperature $T(z=0,t)$ oscillates almost in antiphase to the current at $z=1$.